Published in final edited form as:
*IEEE Trans Neural Syst Rehabil Eng*. 2009 February ; 17(1): 31. doi:10.1109/TNSRE.2008.2008285.

# Medial Gastrocnemius Myoelectric Control of a Robotic Ankle Exoskeleton

**Catherine R. Kinnaird** and
[1]Division of Kinesiology, 401 Washtenaw Ave, Ann Arbor MI, 48109-2013, USA.

**Daniel P. Ferris**
[1]Division of Kinesiology, [2]Department of Biomedical Engineering and [3]Department of Physical Medicine and Rehabilitation, University of Michigan, 1402 Washington Heights, Ann Arbor, MI 48109-2013, USA. (phone: 734-647-6878; fax: 734-647-2808; ferrisdp@umich.edu)

## Abstract

A previous study from our laboratory showed that when soleus electromyography was used to control the amount of plantar flexion assistance from a robotic ankle exoskeleton, subjects significantly reduced their soleus activity to quickly return to normal gait kinematics. We speculated that subjects were primarily responding to the local mechanical assistance of the exoskeleton rather than directly attempting to reduce exoskeleton mechanical power via decreases in soleus activity. To test this observation we studied ten healthy subjects walking on a treadmill at 1.25 m/s while wearing a robotic exoskeleton proportionally controlled by medial gastrocnemius activation. We hypothesized that subjects would primarily decrease soleus activity due to its synergistic mechanics with the exoskeleton. Subjects decreased medial gastrocnemius recruitment by 12% ($p<0.05$) but decreased soleus recruitment by 27% ($p<0.05$). In agreement with our hypothesis, the primary reduction in muscle activity was not for the control muscle (medial gastrocnemius) but for the anatomical synergist to the exoskeleton (soleus). These findings indicate that anatomical morphology needs to be considered carefully when designing software and hardware for robotic exoskeletons.

### Index Terms

Biomechanics; EMG; Gait; Locomotion; Motor Learning

## I. Introduction

Recent advancements in robotics have resulted in prototype powered exoskeletons for assisting human movement. Robotic exoskeletons can be used in rehabilitation to retrain the nervous system to walk [1–5], enhance the abilities of healthy individuals [6–8], and/or help the disabled to live more independently [9–11]. For exoskeletons to be successful in any of these roles, it is critical to understand the human response to various control strategies for powered exoskeletons [12,13].

One control strategy for robotic exoskeletons is proportional myoelectric control. This control method produces a control signal that varies in amplitude proportional to the magnitude of muscle recruitment. In a prior study we found that when subjects walked with soleus proportional myoelectric control of plantar flexor assistance via a robotic ankle exoskeleton, they reached steady state gait dynamics in about 45 minutes [13]. As subjects learned to walk with the exoskeleton, they reduced their soleus electromyography (EMG) amplitude during stance by 37% and returned to a normal walking pattern. There were no significant changes in medial or lateral gastrocnemius EMG amplitudes for the subjects. This study, conducted over

two separate training days, indicated that subjects formed a motor memory of exoskeleton use that could be recalled on future days [13].

Previous studies examining motor learning with brain-machine interfaces have found clear evidence of operant conditioning between the neural control signal and the behavior of the robotic device [14]. This relationship has recently been theoretically outlined in a review by Fetz [15] and promoted as a means to aid neurological rehabilitation by Dobkin [16]. However, there is another means by which a brain-machine interface can indirectly alter neural control signals. The biomechanical effect of a neurally controlled robotic device on movement dynamics (via force and energy transfer) could lead to motor adaptation in muscles other than the muscle supplying the neural control signal. We proposed to test this possibility in the current study.

We used medial gastrocnemius EMG to proportionally control an artificial plantar flexor muscle attached to a custom-built ankle exoskeleton. We replicated the methods of our earlier study [13] with the exception of the muscle used to control the exoskeleton. Medial gastrocnemius is a biarticular muscle that crosses both the ankle joint and the knee joint. The gastrocnemius is not a strict synergist to the artificial plantar flexor on the exoskeleton, so reduction of gastrocnemius muscle activity to decrease robotic plantar flexor assistance would have had mechanical effects at the knee as well as the ankle. We hypothesized that subjects would primarily reduce their soleus activity with practice because the actuator on the exoskeleton was a uniarticular synergist to the soleus. The alternative, in accord with the operant conditioning observed in previous brain-machine interface studies [15], would have been that the nervous system reduced medial gastrocnemius activity because it was the neural control signal responsible for the increased plantar flexor torque. The importance of the study lies in the ability to determine if the nervous system primarily responds by accommodating the biomechanical effects of the robotic exoskeleton in the simplest manner available (i.e. decreasing biological plantar flexor torque without disrupting knee torque).

## II. METHODS

Ten healthy subjects (6 female, 4 male, mean ± standard deviation (SD): age 23.4 ± 3.9 years and mass 68.6 ± 17.6 kg) gave written informed consent and the study protocol was approved by the University of Michigan Institutional Review Board. We used the methods outlined in a previous study [13] except that we substituted medial gastrocnemius EMG for soleus EMG to control the behavior of the artificial pneumatic muscle (i.e. the actuator) on the exoskeleton.

We custom built a unilateral carbon fiber exoskeleton for each subjects' left leg (mean ± SD, mass 1.23 ± 0.12 kg). We chose to fit each subjects' left leg so we could make comparisons with our previous studies. The exoskeleton design has been fully described elsewhere [1,17, 18]. The exoskeletons used in this study are suitable in a research or rehabilitation training environment but are not easily portable due to their dependence on compressed air. They have been used before to study gait in incomplete spinal cord injury subjects [2] and could also be used for stroke and cerebral palsy patients given their dyscoordinated and weak plantar flexion at pushoff. Each exoskeleton is made up of a carbon fiber shank and polypropylene foot section joined by a metal hinge joint allowing rotation about the sagittal plane (Fig. 1).

We attached artificial pneumatic plantar flexor muscles (sometimes called McKibben muscles) to the posterior of the exoskeletons using aluminum brackets (Fig. 1). The artificial muscles are made up of surgical tubing surrounded by braided polyester sheathing. When filled with air the artificial muscles expand and shorten, producing force. Artificial muscle and exoskeleton mechanics have been described in detail [1,17,18].

We wrote custom control software (Simulink, Matlab Inc.) and implemented it using a real-time control board (dSPACE Inc.) to produce a feedforward electrical signal (0 – 10 V) that was proportional to medial gastrocnemius EMG activity. The controlling software recorded the medial gastrocnemius activity, passed the data through a high pass second order Butterworth filter (cutoff frequency 20 Hz), full-wave rectified it, and passed it through a low-pass second order Butterworth filter (cutoff frequency 10 Hz). The control signal activated pressure regulators to control air pressure in the artificial muscles. A manually adjusted threshold value on the control signal ensured that background EMG noise did not activate the artificial muscle during the swing phase. The gain of the control signal was manually adjusted to use the full 10 V range based on the EMG pattern during unassisted walking [13]. Gain and threshold values were tuned manually for each subject during walking with the unpowered exoskeleton by viewing the control signal on a computer display. The same subject tuned gain and threshold values for all subjects.

For all experiments, subjects walked on a treadmill at 1.25 m/s while we recorded kinematic, kinetic and EMG data. We used an eight camera system (Motion Analysis Corporation, Santa Rosa, CA) and reflective markers on the lower limbs to collect kinematic data. Step-cycle data were collected with footswitches placed in the subjects' shoes. A load cell (1200 Hz, Omega Engineering) monitored the force produced by the artificial muscle. We recorded EMG signals (1200 Hz, Konigsberg Instruments Inc.) using bipolar surface electrodes on medial gastrocnemius, soleus, lateral gastrocnemius, tibialis anterior, vastus lateralis, vastus medialis, rectus femoris and medial hamstring.

Subjects underwent two identical testing sessions three days apart. Subjects walked on a treadmill while wearing the exoskeletons passive for 10 minutes (baseline), powered for 30 minutes (powered) and passive for 15 minutes (post) (Fig. 1). Subjects made all transitions from passive to powered and powered to passive while walking. We gave subjects a verbal warning before the transitions for safety. Subjects were instructed to walk how they were most comfortable.

We collected data from the first 10 seconds of every minute of treadmill walking. We created step-cycle profiles for the kinematic, kinetic and EMG data from left heel strike to left heel strike for each subject. Average step-cycle profiles were calculated using all complete steps recorded during each 10-second interval. By calculating normalized EMG root mean squared values we were able to examine differences in EMG amplitude with training. We high pass filtered (second order Butterworth filter, cutoff frequency 20 Hz) and full-wave rectified EMG data to calculate root mean squared values for all signals during the stance phase of each step, and over the entire gait cycle. We normalized EMG root mean squared values to the average EMG root mean squared value of the 10-second interval of the last minute of passive walking. Joint angle step cycle profiles were created from smoothed kinematic data (low pass, second order Butterworth filter, cutoff frequency 6 Hz) using Visual3D software (C-Motion Inc.). We used the averaged joint angle step cycle profiles of the ankle, knee, and hip to calculate Pearson product moment correlations for each minute of active walking versus the last minute of baseline walking. The $r^2$ values from the correlations allowed us to determine how closely the subjects' kinematics profiles were to baseline. We used the load cell data and ankle kinematics to calculated exoskeleton torque and power about the ankle, as well as exoskeleton positive and negative work.

We used repeated measure ANOVAs to test for differences between days and conditions (baseline minute 10 passive walking, powered minutes 1, 15 and 30, post passive walking minutes 1 and 15) in joint angle correlation common variance, positive and negative work, and normalized EMG root mean squared values ($P<0.05$ as significance level) with Tukey honestly (THSD) post hoc tests where appropriate.

In order to evaluate adaptation rates we calculated how long it took subjects to reach the steady state envelope using the method outlined previously [13,19]. We defined the powered exoskeleton steady state envelope as the mean value for each metric ±2 SD of the average of the last 15 minutes of day 2 powered walking. The metric was said to have entered steady state after at least 3 consecutive minutes of values entering the envelope and no more than 1 consecutive value falling outside the envelope for the duration of the powered testing. We calculated the steady state envelope for determining post adaptation rates by using mean ±2 SD of 10 minutes of passive walking which included the last 5 minutes of baseline walking and the last 5 minutes of post walking.

In order to estimate how much assistance the exoskeleton was providing, nine of the subjects return for a third day of testing (the tenth subject relocated and was not available). The subjects walked over static force plates at 1.25 m/s. These data allowed us to calculate biological ankle work and power (Visual3d, C-Motion, Inc.). The lower limb inertial properties were assumed based on anthropometric measurements of the subjects [20].

## III. RESULTS

### A. Day 1, Powered Minute 1

When the power to the exoskeleton was turned on, subjects underwent a marked change in kinematics and EMG. Due to the large increase in plantar flexor torque assistance provided, subjects initially walked on their forefoot and toes, with no heel contact. Peak plantar flexion angle increased, from 13.8±4.7° during baseline walking to 25.8±7.6° during the first minute of powered walking (Fig. 2). Consequently, we observed the lowest ankle angle common variance value with respect to baseline from all testing days ($r^2$ = 0.52±0.26). Knee and hip kinematics changes were not as marked as for the ankle, with common variances of 0.80±0.30 and 0.97±0.02, respectively (Fig. 3).

We observed a change in biological muscle activity in all muscles (Fig. 4). Tibialis anterior, medial gastrocnemius, lateral gastrocnemius, vastus lateralis, rectus femoris and medial hamstring all had significantly higher EMG root mean squared values during stance with respect to baseline. Soleus and vastus medialis stance root mean squared values during the first minute of powered walking were not significantly different than baseline. There was almost constant activation in medial gastrocnemius during the first powered minute (Fig. 5). The increased medial gastrocnemius activity caused an increase in exoskeleton torque throughout the gait cycle (Fig. 6). This resulted in negative exoskeleton mechanical power at the beginning of stance and positive mechanical power at the end of stance (Fig. 6).

### B. Day 1, Powered Minute 30

Subjects were able to adapt over the 30-minute training session in order to walk comfortably and more normally, when compared to baseline. The peak plantar flexion angle was reduced to 18.7±7.0°which was significantly different from the first minute of powered walking (Fig. 2). However, ankle angle common variance during the last minute of powered walking ($r^2$=0.76 ±0.14) was still significantly different from baseline passive walking. The ankle common variance adaptation period was 25±8 minutes. By the end of the first powered session knee and hip common variances increased to 0.95±0.05 and 0.98±0.02 respectively, and were not significantly different from baseline (Fig. 3). EMG activity returned to close to normal bursting patterns by the end of the 30 minute session. All EMG root mean squared values, except soleus, were not significantly different from baseline after 30 minutes of walking. At the 30$^{th}$ minute of powered walking soleus EMG root mean squared amplitude was reduced by 18% (Fig. 7). The medial gastrocnemius EMG RMS adaptation period was 21.6±11.0 minutes and the soleus stance EMG RMS adaptation period was 19.1±11.5 minutes (Fig. 8). Soleus and medial

gastrocnemius EMG root mean squared values at minute 30 were not significantly different than the values at minute 15. There was a significant decrease in negative exoskeleton mechanical work from minute 1 to minute 15 and no significant difference in positive exoskeleton mechanical work at minute 1, 15, and 30 (Fig. 9).

### C. Day 2, Powered Minute 1

Subjects experienced a less marked change in kinematics, kinetics and biological EMG levels during the first minute of day 2 when compared to day 1. There was a significant increase in peak plantar flexion angle, from 14.6±4.0° at baseline to 19.2±8.1° (Fig. 2). Ankle angle common variance was 15% higher during the first minute of day 2 powered walking than the first minute of day 1 powered walking. Ankle and knee angle common variances were significantly different than baseline, but not different than the first minute of day 1 powered walking. Hip common variance was not significantly different from baseline during the first minute of powered walking (Fig. 3).

There was an increase in muscle activity during the 1$^{st}$ minute of powered walking, although not to the extent seen on day 1 (Fig. 4). Medial gastrocnemius and soleus immediately exhibited clear bursting patterns (Figs. 4 and 6). Medial gastrocnemius stance root mean squared values were significantly less than both the 1$^{st}$ and 30$^{th}$ minutes of day 1 powered walking (Fig. 5). Positive and negative mechanical work was not significantly different from the 1$^{st}$ and 30$^{th}$ minutes of day 1 powered walking (Fig. 9).

### D. Day 2, Powered Minute 30

Subjects returned to normal kinematics with practice, as compared to baseline, within 6.2±5 minutes (Fig. 8). Ankle angle common variance increased to 0.86±0.17, which was not significantly different from baseline. Knee and hip common variances were also not significantly different from the last minute of day 1, baseline of day 2 or the first minute of day 2 (Fig. 3).

Medial gastrocnemius EMG root mean squared values during stance at minute 30 of day 2 powered walking was significantly less than the first minutes of both day 1 and day 2 (Fig. 5). Soleus stance root mean squared values were significantly lower than the first minute of day 1, but not different than the first powered minute of day 2 (Fig. 7).

Compared with baseline, medial gastrocnemius activity decreased by 12% and soleus activity decreased by 26%. Medial gastrocnemius and soleus adaptation periods for day 2 were 5.1±5.4 minutes and 3.6±5.4 minutes, respectively (Fig. 8). All other muscle EMG root mean squared values were not significantly different from baseline at minute 15 or minute 30. There was no significant change in exoskeleton positive or negative mechanical work from minute 1 to minute 30 (Fig. 9).

## IV. DISCUSSION

While most results from this study are qualitatively similar to the previous study using soleus proportional myoelectric control [13], the changes in triceps surae EMG amplitudes with training were very illuminating. In the present study, subjects significantly decreased their medial gastrocnemius EMG (providing the control signal) by 12% but significantly decreased soleus EMG by 27%. In the Gordon and Ferris (2007) study [13], soleus EMG (providing the control signal) decreased by 35% while medial gastrocnemius was not significantly different after adaptation. These results support our hypothesis that the nervous system primarily adapts to the biomechanical effect of the robotic exoskeleton in the simplest manner.

There was a small amount of concomitant reduction in medial gastrocnemius EMG when it was used as the control signal. This suggests that the nervous system did learn the associative relationship between medial gastrocnemius muscle activity and the mechanical response of the exoskeleton to a certain extent. There is likely a small range of gastrocnemius torque reduction that would not substantially alter knee joint kinetics due to the other muscles providing knee flexor torque. By reducing gastrocnemius activation slightly, the nervous system gained a double decrease in plantar flexor torque (both biological and artificial muscles produced less joint torque) with only a small decrease in knee flexor torque.

Although soleus and medial gastrocnemius muscles both provide plantar flexor torque, they are not true synergists during human walking. The medial gastrocnemius is a biarticular muscle that can be considered a knee flexor as well as an ankle plantar flexor. Unlike the soleus, its activation is dependent on the position of the knee [21,22]. A recent study using electrical stimulation to examine differences in biomechanical roles for the gastrocnemius and soleus [23] found clear functional separation between the two muscles. Those empirical results agree with findings from musculoskeletal computer simulations of human walking highlighting a clear difference in the functional effects of the two triceps surae muscles [24].

The primary activation reduction in the soleus in the current study suggests that the nervous system reacted to the powered exoskeleton based on the mechanical output of the exoskeleton (energy and torque transfer to the human). The main reduction in activation was not in the muscle providing the control signal. This finding has important implications for using proportional myoelectric control in robotic exoskeletons. Designers of exoskeletons need to consider muscle anatomy when they choose actuator attachment locations and torque capabilities for assisting human movement. Many robotic exoskeletons rely on torque motors at the joints (uniarticular assist) that are not anatomically biomimetic. The resulting changes in muscle recruitment and mechanics may not be what were originally intended by the engineer. The human body relies on both uniarticular and biarticular muscles to produce a remarkably economical and coordinated gait. Future robotic exoskeletons may benefit from using linkages that couple joint dynamics in a more biomimetic manner. Given the importance of biarticular muscles in movement economy, stabilization, and limb force direction [25–27], a robotic lower limb exoskeleton with biarticular muscles might surpass exoskeletons using rotational torque motors in performance.

There were no substantial differences in adaptation rates for the current study and the previous one by Gordon and Ferris (2007). In this study, the adaptation rate for the first training day was 25 minutes for ankle kinematics and 22 minutes for medial gastrocnemius EMG. These are similar to the respective values in the soleus control study (24 minutes for ankle kinematics and 24 minutes for soleus EMG). By the second training day in both studies, these adaptation rates all dropped to less than 6 minutes. These results indicate that neurologically intact humans are able to learn effective control of the exoskeleton within similar time periods regardless of the ankle plantar flexor chosen to control the exoskeleton. This is somewhat surprising in that it has been suggested that pure extensor muscles like the soleus may be more directly tied to central pattern generator output and less mutable than biarticular muscles like the medial gastrocnemius [28,29]. Similar adaptation rates were also demonstrated by neurologically intact subjects adapting to a bang-bang kinematic control method for the robotic ankle exoskeleton [12]. This suggests there may be a similar adaptation period to an exoskeleton based on the hardware rather than the control approach. Future studies of robotic lower limb exoskeletons should measure adaptation periods for better reference.

## V. Conclusion

Previous studies of motor learning with brain-machine interfaces have found that the primary neural adaptation is in the neural signal used to control the robotic device [15]. However, these devices are typically not mechanically interfaced with the body of the human or animal. We speculated that a robotic device that was mechanically coupled to a human could produce substantial alterations in muscle activation signals not used for control of the robotic device. We replicated a previous study with the modification of using EMG from a biarticular muscle (medial gastrocnemius) to control a robotic ankle exoskeleton instead of EMG from a uniarticular muscle (soleus). In agreement with our hypothesis, the primary reduction in muscle activity was not for the control muscle (medial gastrocnemius) but for the anatomical synergist to the artificial plantar flexor (soleus). This suggests that the nervous system adapted to the powered assistance primarily to alleviate the increased plantar flexor torque provided by the exoskeleton. This study is the first clear demonstration of how mechanical energy transfer from a robotic device to a person via a neuroelectrical interface can result in primary motor pattern adaptations other than modification of the neural control signal. This finding suggests that neuroelectrical control of robotic devices could be a productive tool for promoting motor adaptation in humans.

## Acknowledgments

This work was supported by NIH R01 NS045486.

We thank members of the Human Neuromechanics Laboratory for assistance in collecting data, and Jake Godak and Anne Manier for fabricating portions of the exoskeletons.

## VI. REERENCES

1. Ferris DP, Sawicki GS, Domingo A. Powered lower limb orthoses for gait rehabilitation. Topics in Spinal Cord Injury Rehabilitation 2005;11:39–49.
2. Sawicki GS, Domingo A, Ferris DP. The effects of powered ankle-foot orthoses on joint kinematics and muscle activation during walking in individuals with incomplete spinal cord injury. Journal of Neuroengineering and Rehabilitation 2006;3:3. [PubMed: 16504172]
3. Colombo G, Wirz M, Dietz V. Driven gait orthosis for improvement of locomotor training in paraplegic patients. Spinal Cord 2001;39:252–255. [PubMed: 11438840]
4. Agrawal SK, Banala SK, Fattah A, Sangwan V, Krishnamoorthy V, Scholz JP, Hsu WL. Assessment of motion of a swing leg and gait rehabilitation with a gravity balancing exoskeleton. IEEE Transactions of Neural Systems and Rehabilitation Engineering 2007;15:410–20.
5. Veneman JF, Kruidhof R, Hekman EE, Ekkelenkamp R, Van Asseldonk EH, van der Kooij H. Design and evaluation of the LOPES exoskeleton for interactive gait rehabilitation. IEEE Transactions on Neural Systems and Rehabilitation Engineering 2007;15:379–86. [PubMed: 17894270]
6. Walsh C, Endo K, Herr H. A quasi-passive leg exoskeleton for load carrying augmentation. International Journal of Humanoid Robotics 2007;4:487–506.
7. Kazerooni H, Steger R. The Berkeley Lower Extremity Exoskeleton. Journal of Dynamic Systems Measurement and Control-Transactions of the ASME 2006;128:14–25.
8. Zoss AB, Kazerooni H, Chu A. Biomechanical Design of the Berkeley Lower Extremity Exoskeleton (BLEEX). IEEE/ASME Transactions on Mechatronics 2006;11:128–138.
9. Kawamoto, H.; Sankai, Y. Comfortable power assist control method for walking aid by HAL-3. IEEE International Conference on Systems, Man and Cybernetics; 2002. p. 1-6.
10. Suzuki, K.; Kawamura, Y.; Hayashi, T.; Sakurai, T.; Hasegawa, Y.; Sankai, Y. Intention-based walking support for paraplegia patient. IEEE International Conference on Systems, Man and Cybernetics; 2005. p. 2707-2713.

11. Blaya JA, Herr H. Adaptive control of a variable-impedence ankle-foot orthosis to assist drop-foot gait. IEEE Transactions on Neural Systems and Rehabilitation Engineering 2004;12:24–31. [PubMed: 15068184]
12. Cain SM, Gordon KE, Ferris DP. Locomotor adaptation to a powered ankle-foot orthosis depends on control method. Journal of Neuroengineering and Rehabilitation 2007;4:48. [PubMed: 18154649]
13. Gordon KE, Ferris DP. Learning to walk with a robotic ankle exoskeleton. Journal of Biomechanics 2007;40:2636–44. [PubMed: 17275829]
14. Lebedev MA, Nicolelis MA. Brain-machine interfaces: past, present and future. Trends in Neuroscience 2006;29:536–46.
15. Fetz EE. Volitional control of neural activity: implications for brain-computer interfaces. Journal of Physiology (London) 2007;579:571–9. [PubMed: 17234689]
16. Dobkin BH. Brain-computer interface technology as a tool to augment plasticity and outcomes for neurological rehabilitation. Journal of Physiology (London) 2007;579:637–42. [PubMed: 17095557]
17. Ferris DP, Gordon KE, Sawicki GS, Peethambaran A. An improved powered ankle-foot orthosis using proportional myoelectric control. Gait and Posture 2006;23:425–8. [PubMed: 16098749]
18. Gordon KE, Sawicki GS, Ferris DP. Mechanical performance of artificial pneumatic muscles to power an ankle-foot orthosis. Journal of Biomechanics 2006;39:1832–41. [PubMed: 16023126]
19. Noble JW, Prentice SD. Adaptation to unilateral change in lower limb mechanical properties during human walking. Experimental Brain Research 2006;169:482–95.
20. Zatsiorsky, VM. Kinetics of Human Motion. Champaign, IL: Human Kinetics; 2002.
21. Sale D, Quinlan J, Marsh E, McComas AJ, Belanger AY. Influence of joint position on ankle plantarflexion in humans. J Appl Physiol 1982;52:1636–42. [PubMed: 7107473]
22. Cresswell AG, Loscher WN, Thorstensson A. Influence of gastrocnemius muscle length on triceps surae torque development and electromyographic activity in man. Experimental Brain Research 1995;105:283–90.
23. Stewart C, Postans N, Schwartz MH, Rozumalski A, Roberts A. An exploration of the function of the triceps surae during normal gait using functional electrical stimulation. Gait and Posture 2007;26:482–8. [PubMed: 17223346]
24. Neptune RR, Kautz SA, Zajac FE. Contributions of the individual ankle plantar flexors to support, forward progression and swing initiation during walking. Journal of Biomechanics 2001;34:1387–98. [PubMed: 11672713]
25. Neptune RR, Sasaki K, Kautz SA. The effect of walking speed on muscle function and mechanical energetics. Gait Posture 2008;28:135–43. [PubMed: 18158246]
26. van Ingen Shenau GJ. Proposed actions of bi-articular muscles and the design of hindlimbs of bi- and quadrupeds. Human Movement Science 1994;13
27. van Ingen Shenau GJ. On the action of bi-articular muscles, a review. Netherlands Journal of Zoology 1990;40:521–540.
28. English AW, Weeks OI. An anatomical and functional analysis of cat biceps femoris and semitendinosus muscles. Journal of Morphology 1987;191:161–75. [PubMed: 3560234]
29. Pratt CA, Buford JA, Smith JL. Adaptive control for backward quadrupedal walking V. Mutable activation of bifunctional thigh muscles. Journal of Neurophysiology 1996;75:832–42. [PubMed: 8714656]

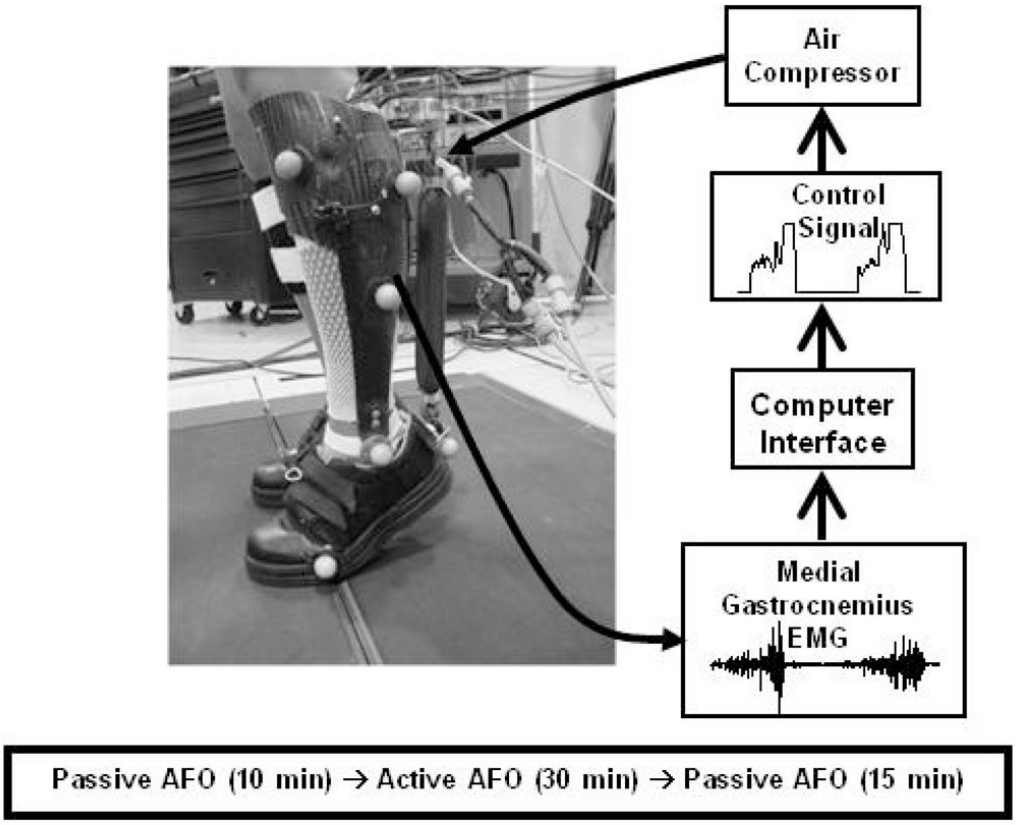


**Fig. 1.**
Custom fit robotic ankle exoskeleton experimental setup and control algorithm. The exoskeletons were powered with an artificial plantar flexor that expanded and shortened when filled with air, proportional to medial gastrocnemius EMG.

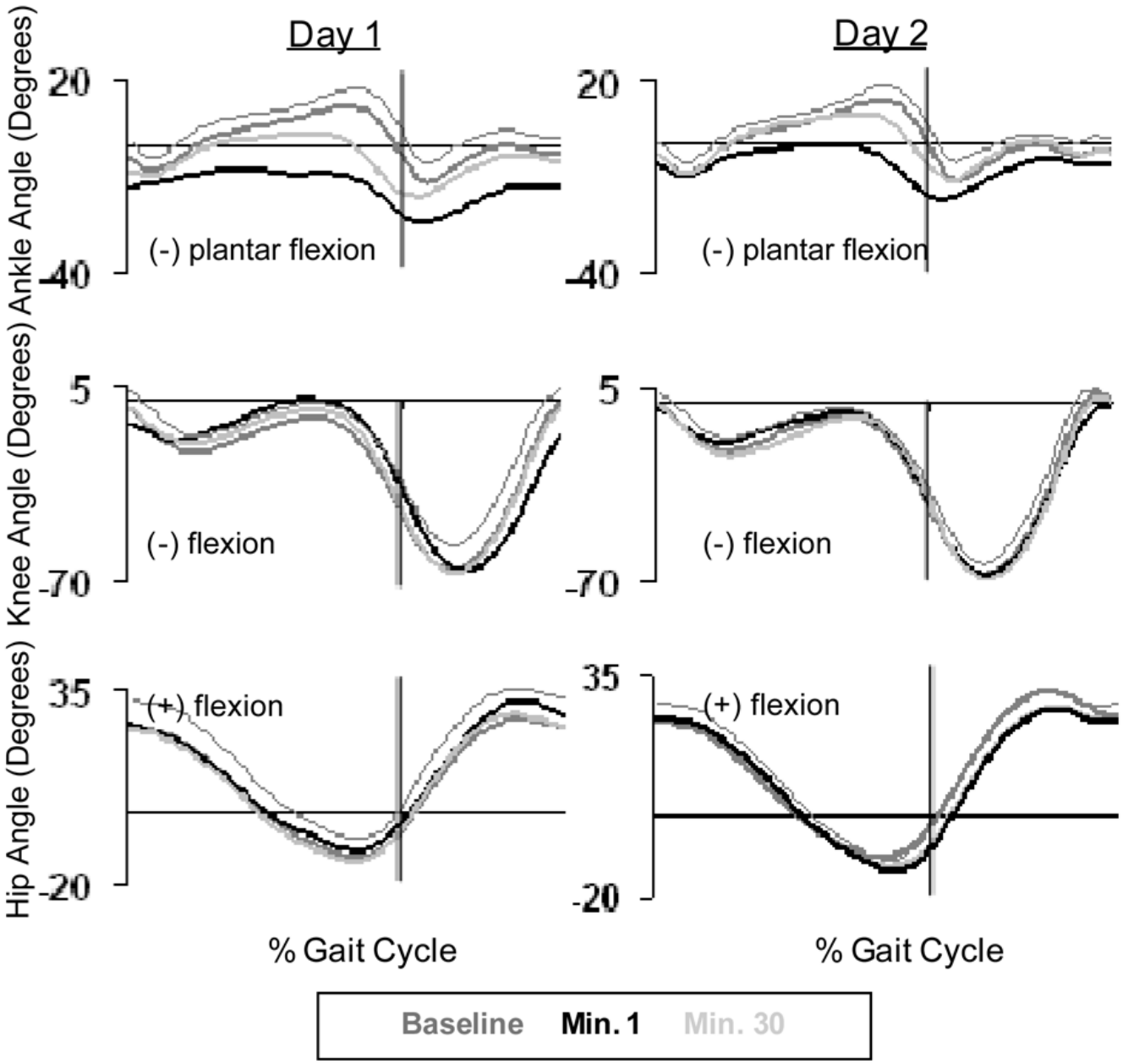


**Fig. 2.**

Ankle, knee, and hip angle kinematic patterns averaged for all subjects (n=10) across the gait cycle. Baseline data (dark grey line), powered minute 1 (black line), and powered minute 30 (grey line) are given for day 1 and day 2.

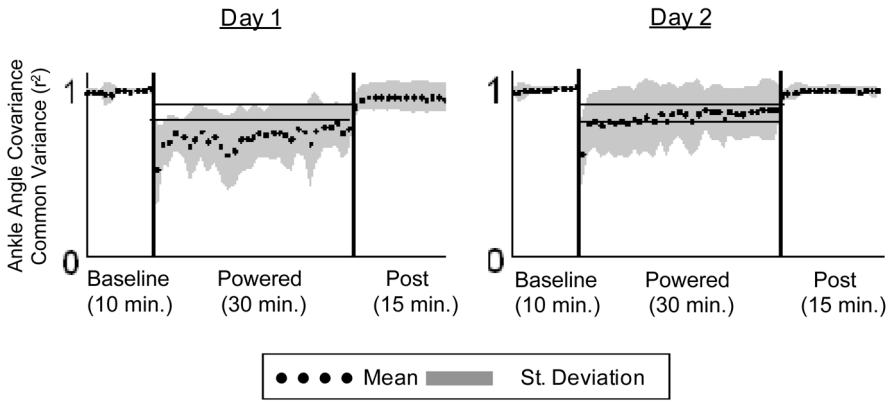


**Fig. 3.**

Ankle joint Pearson product moment correlation values ($r^2$) for each minute of walking with respect to baseline. Mean (black dots) +/− SD (grey area) of all subjects (n=10). The horizontal black lines show +/− 2 standard deviations of group mean data from the last 15 min of day 2, representing steady state dynamics. These steady state envelopes are calculated from group mean data and are for display purposes only. Individual subject analyses were used for statistical tests.

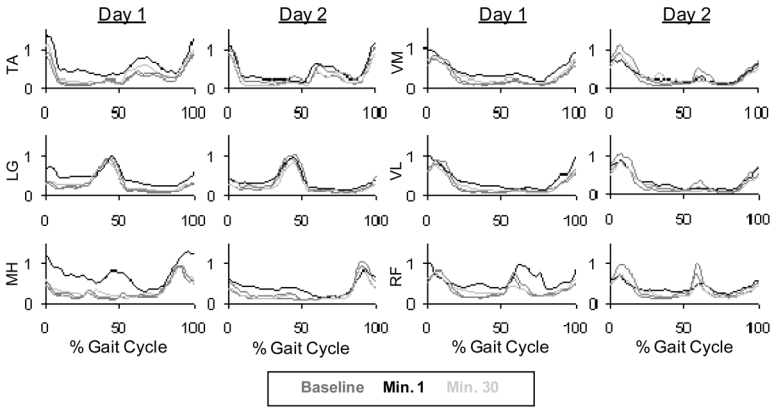


**Fig. 4.**

Lower leg EMG linear envelopes for day 1 and day 2 (Butterworth low-pass filter with zero lag and cutoff of 10 Hz. Tibialis anterior (TA), lateral gastrocnemius (LG), medial hamstring (MH), vastus medialis (VM) and vastus lateralis (VL), are averaged for the entire gait cycle across subjects. Due to missing data there were between 8 and 10 subjects per muscle group (n=10, 9, 9, 8, 8, 9 respectively.

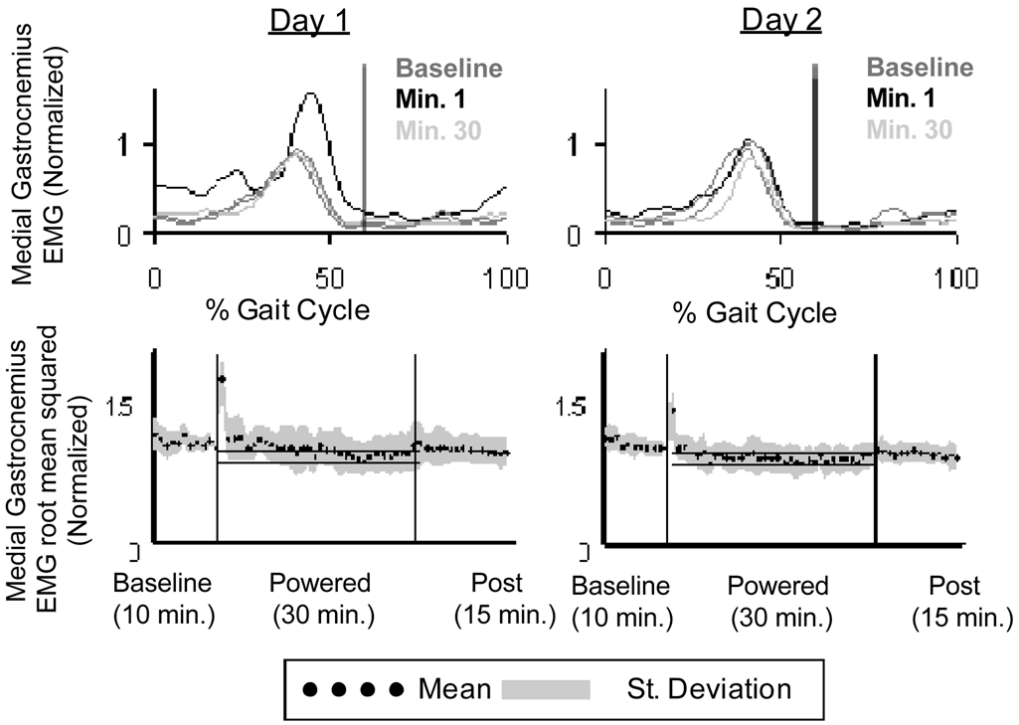


**Fig. 5.**

(a) Medial gastrocnemius EMG linear envelopes for day 1 and day 2 (Butterworth low-pass filter with zero lag and cutoff of 10 Hz) averaged across all subjects (n=10). Vertical black lines indicate toe-off. (b) Medial gastrocnemius root mean squared data averaged (black dots) for all subjects (grey area is +/− 1 SD) for each minute of walking with the exoskeleton. The horizontal black lines show +/− 2 standard deviations of group mean data from the last 15 min of day 2, representing steady state dynamics. These steady state envelopes are calculated from group mean data and are for display purposes only. Individual subject analyses were used for statistical tests.

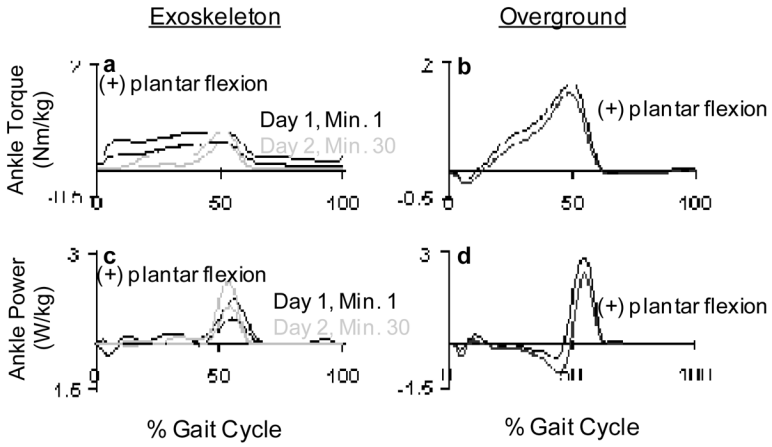


**Fig. 6.**

(a) Exoskeleton plantar flexor torque from day 1 (black line) and day 2 (grey line). (b) Plantar flexion torque produced at the ankle during overground walking without wearing an exoskeleton. (c) Averaged exoskeleton power produced at the ankle from day 1 (black line) and day 2 (grey line). (d) Ankle power produced at the ankle during overground walking without wearing an exoskeleton. The bold lines represent averaged data from 9 subjects, and thin lines represent +1 SD.

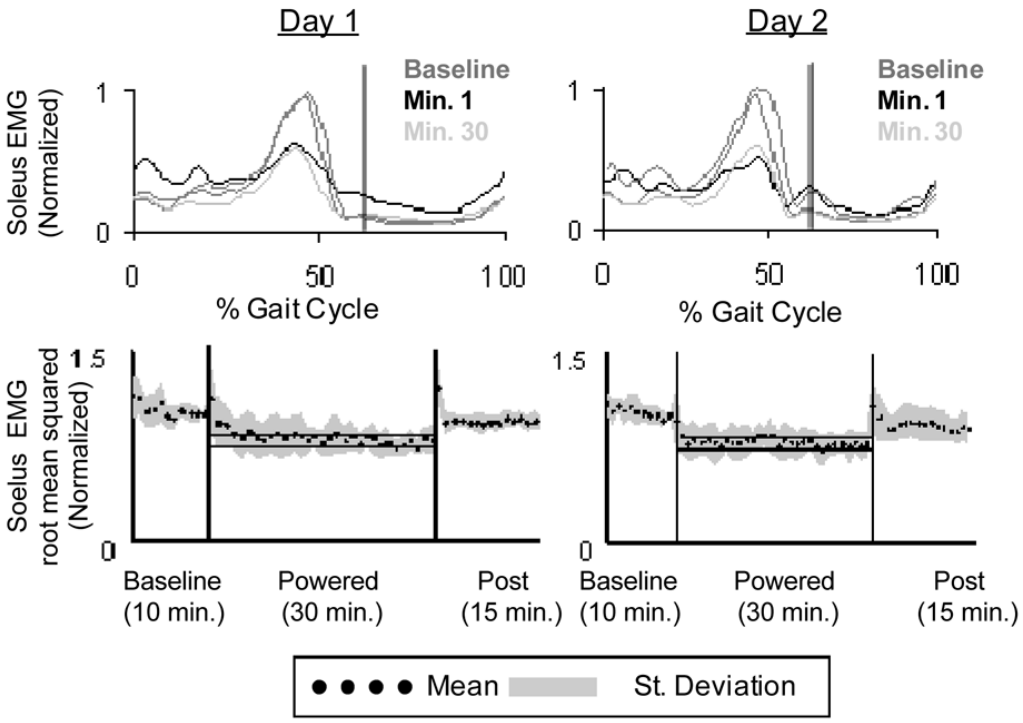


**Fig. 7.**

(a) Soleus EMG linear envelopes for day 1 and day 2 (Butterworth low-pass filter with zero lag and cutoff of 10 Hz) averaged across 8 subjects. Vertical black lines indicate toe-off. (b) Soleus root mean squared data averaged (black dots) across 8 subjects (grey area is +/− 1 SD) for each minute of walking with the exoskeleton. The horizontal black lines show +/− 2 standard deviations of group mean data from the last 15 min of day 2, representing steady state dynamics. These steady state envelopes are calculated from group mean data and are for display purposes only. Individual subject analyses were used for statistical tests.

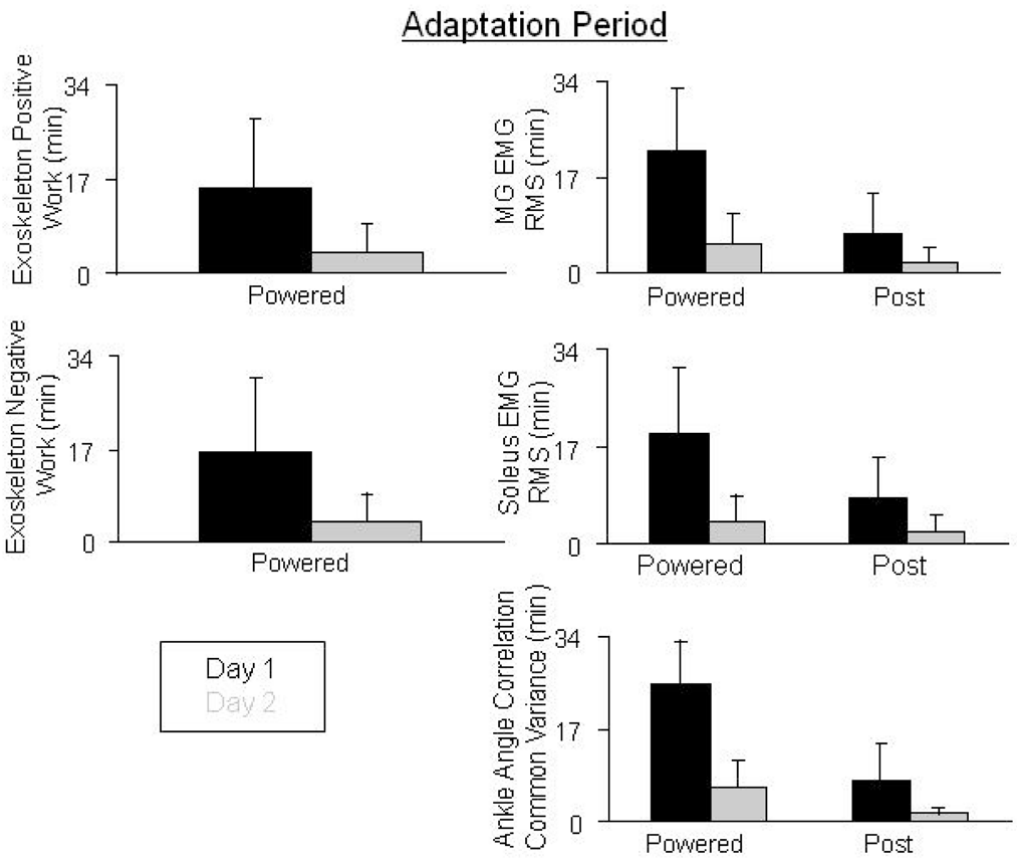


**Figure 8.**

Adaptation times for day 1 (black) and day 2 (grey) for exoskeleton positive and negative work, medial gastrocnemius and soleus EMG root mean square, and ankle correlation common variances. Data represent averages across subjects +1 SD.

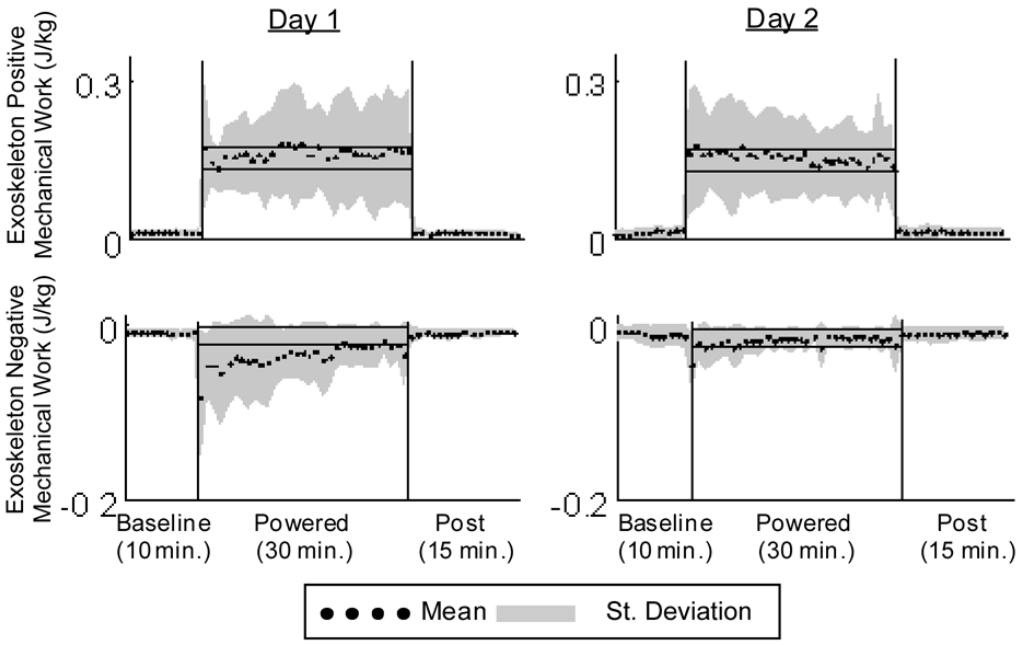


**Figure 9.**

Positive and negative exoskeleton mechanical work (J/kg) averaged across 9 subjects (black dots) +/− 1 SD (grey area). Positive mechanical work stays constant over day 1 and day 2 while there is a substantial decrease in exoskeleton negative work on both day 1 and day 2. The horizontal black lines show +/− 2 standard deviations of group mean data from the last 15 min of day 2, representing steady state dynamics. These steady state envelopes are calculated from group mean data and are for display purposes only. Individual subject analyses were used for statistical tests.